JCTC Journal of Chemical Theory and Computation

Quantum Dynamics of Electron Transfer from Bacteriochlorophyll to Pheophytin in Bacterial Reaction Centers†

Raffaele Borrelli, Mariangela Di Donato,‡ and Andrea Peluso*

Dipartimento di Chimica, Università di Salerno, Fisciano (SA), I-84081, Italy

Received December 28, 2006

Abstract: We extend our previous works on the early electron-transfer steps in bacterial photosynthetic reaction centers to the dynamics of electron transfer from the bacteriochlorophyll anion to pheophytin. The approach employed here takes into account the whole set of normal coordinates of the acceptor and donor groups, in order to reliably account both for shifts and mixing of the normal coordinates and for changes in vibrational frequencies upon electron transfer. It is shown that intramolecular modes provide not only a discrete set of states strongly coupled to the initial state but also a quasi-continuum of weakly coupled states, which account for faster dephasing effects. Detuning effects are accounted for by averaging the computed probability over a small range of the electronic energy difference. The computed transition probability is of the same order of magnitude, a few picoseconds, as the observed one.

1. Introduction

Long-range electron transfer (ET) is an important process for energy transduction in living systems. The high structural complexity of the natural energy transducers, for example the photosynthetic reaction centers (PRC), suggests that the efficiency of the energy conversion should result from the interplay of several structural effects.[1,2] A better understanding of that interplay is desirable not only for scientific purposes but also for technological progress, particularly in the area of supramolecular chemistry involved in the design of molecular machines capable of performing similar operations.[3−7]

The basic concepts for understanding ET processes in condensed media have been provided by Marcus' theory and its quantum extensions,[8−11] which have the great merit of having individuated the most important physicochemical factors which affect ET rates: the intramolecular and intermolecular reorganization energies, which depend on the relative displacements of the equilibrium geometries of the two electronic states, the Gibbs' free energy change upon ET, the Franck−Condon (FC) factors, and the electronic coupling term.

The comprehension of a specific ET mechanism is thus realized in the ability of associating the above quantities, and then ET rates, to the specific physicochemical properties of the single molecular components and of the supramolecular structure of the whole system. A first difficulty arises already at the stage of disentangling all the above quantities from experimental data. That step would require the detailed knowledge of the normal modes of vibration and of their changes upon ET, namely, how they are displaced and/or rotated upon ET, and these data cannot be easily obtained from experimental data.[12,13]

Because of the lack of specific information about modes which are displaced and/or rotated upon ET, in the past, a single intramolecular mode coupled to a continuum provided by the modes of a thermal bath (the surrounding medium) served as the reference model for the effect of intramolecular vibrations in ET dynamics,[14] but there are reasons to believe that, although fluctuations introduced by the pertinent interactions of the main ET cofactors with the environments are certainly important for ET, the assumption of a single quantum mode could compromise the ability of extracting

† Dedicated to Professor Dennis R. Salahub on the occasion of his 60th birthday.

* Corresponding author e-mail: apeluso@unisa.it.

‡ Present address: Department of Physics and Astronomy, Faculty of Sciences, Free University, 1081 HV Amsterdam, The Netherlands.

10.1021/ct6003802 CCC: $37.00
Published on Web 04/04/2007

from the experimental data all the parameters which control ET.[12] Furthermore, since with only one or even a few discrete modes it is impossible to achieve the degeneracy conditions required for tunneling, those simplified models have led to assign to the classical motion of the surrounding medium a more important role than it might deserve.

Clearly, the possibility of building a more satisfactory model depends on the availability of detailed data concerning the energies and the mutual couplings of the vibronic states involved in ET. Theoretical computations can be of great help in giving reliable estimates of at least a part of the above quantities.[15] In particular, methods based on density functional theory (DFT), a field in which Dennis Salahub has been undoubtedly a pioneer,[16−19] turned out to be highly reliable in predicting both vibrational frequencies and electronic excitation energies, which are both of primary interest in the analysis of ET rates.

In this paper, we will use the results of DFT computations to characterize the vibronic states of bacteriochlorophyll and bacteriopheophytin, two redox cofactors of the ET chain in bacterial PRCs, and to study the dynamics of the ET process, with the attempt of better clarifying the role of B_A in the ET chain of bacterial PRCs. In fact, the involvement of the monomer bacteriochlorophyll B_A as an intermediate electron acceptor, leading to the formation of the charge separate state $P^+B_A^-$, has been debated for a long time in the literature, probably because the characteristic absorption region for the monomer bacteriochlorophyll, around 800 nm, is highly congested.

The excited state of P* has a lifetime of ca. 3 ps; within this time interval, spectral features attributable to the formation of the bacteriopheophytin anion (H_A^-) can be identified. Early time-resolved pump−probe measurements, probing the region of the bleaching of the ground-state absorption of P (870 nm) and that of H_A (545 nm) and the appearance of the bacteriopheophytin anion (660 nm), gave no indication of the involvement of an intermediate electron acceptor.[20] It was concluded that the presence of B_A served to facilitate the direct electron transfer between P and H_A via a superexchange ET mechanism. Subsequent measurements, probing the spectral region in which the anion of the monomer bacteriochlorophyll is expected to absorb (1020 nm), gave an indication for the formation of the charge-separated state $P^+B_A^-$, which occurs with a time constant of ca. 1 ps.[21] The results reported in this paper support these experimental findings showing that the $P^+B_A^-$ intermediate rapidly undergoes ET to H_A in ca. 0.5−2 ps, in good agreement with the observed decay time.

2. ET Dynamics

Basic concepts. Our approach to ET dynamics is based on the standard treatment of radiationless processes.[22] Here, we rapidly illustrate the basic concepts for the case where ET involves only two molecules, an acceptor *A* and a donor *D*. The electronic wavefunctions of this system can be expressed as the superposition of two diabatic states $|AD^-\rangle \equiv |D\rangle$ and $|A^-D\rangle \equiv |A\rangle$, representing electronic states with the negative charge fully localized on one of the two partners.

On the condition that all other states of the systems are well-separated in energy, $|D\rangle$ and $|A\rangle$ form a complete and linearly independent orthonormal basis for the lower-energy electronic states of *A* and *D*. Each of the two electronic diabatic states is characterized by a manifold of vibronic states, which can also be grouped in two subsets, denoted $\overline{|D\rangle}$ and $\overline{|A\rangle}$.

In the Born−Oppenheimer approximation, the elements of $\overline{|D\rangle}$ and $\overline{|A\rangle}$ are given by the direct product of the electronic and vibrational wavefunctions:

$$|A, \bar{v}\rangle = |\psi_A\rangle \otimes |\bar{v}_A\rangle, |D, \bar{w}\rangle = |\psi_D\rangle \otimes |\bar{w}_D\rangle \qquad (1)$$

where $\bar{v}$ and $\bar{w}$ denote the set of the vibrational quantum numbers associated to each normal mode of vibration.

Any state of the system can then be written as a linear combination of the elements of the two state manifolds:

$$|\Psi(t)\rangle = \overline{|A\rangle}\,\mathbf{C}_A(t) + \overline{|D\rangle}\,\mathbf{C}_D(t) \qquad (2)$$

where $\mathbf{C_A}$ and $\mathbf{C_D}$ are column vectors, whose sizes are given by the dimensions of the vibrational subspaces of $\overline{|A\rangle}$ and $\overline{|D\rangle}$ considered relevant to the problem under consideration.

The expansion coefficients $\mathbf{C}(t)$ of eq 2 determine the time evolution of $|\Psi(t)\rangle$ and therefore the dynamics of ET; they are solutions of the time-dependent Schrödinger equation:

$$-i\hbar\begin{pmatrix}\dot{\mathbf{C}}_A(t)\\ \dot{\mathbf{C}}_D(t)\end{pmatrix} = \begin{pmatrix}\mathbf{H_{AA}} & \mathbf{H_{AD}}\\ \mathbf{H}_{AD}^{\dagger} & \mathbf{H_{DD}}\end{pmatrix}\begin{pmatrix}\mathbf{C_A}\\ \mathbf{C_D}\end{pmatrix} \qquad (3)$$

with initial conditions specifying the initial state of the system. Each of the four matrix blocks in eq 3 is a matrix whose size depends on the number of vibrational states belonging to $\overline{|A\rangle}$ and $\overline{|D\rangle}$. Since the off-diagonal elements are in general nonvanishing, the elements of $\overline{|A\rangle}$ and $\overline{|D\rangle}$ are not eigenstates of the Hamiltonian operator and change in time.

The matrix elements of the diagonal and extradiagonal blocks of **H** are

$$H_{A\bar{w}A\bar{v}} = \langle A\bar{v}|\mathscr{H}^{\mathrm{el}} + \mathscr{T}_N|A\bar{w}\rangle = \langle \bar{v}_A|\mathscr{E}_A(R) + \mathscr{T}_N|\bar{w}_A\rangle = E^{\mathrm{tot}}_{A\bar{v}}\delta_{\bar{w},\bar{v}} \qquad (4)$$

where $\mathscr{E}_A(r)$ is the nuclear potential energy operator of $\overline{|A\rangle}$

$$H_{\mathrm{A}\bar{w}D\bar{v}} = \langle A\bar{v}|\mathscr{H}^{el} + \mathscr{T}_N|D\bar{w}\rangle = \langle \bar{v}_A|\lambda(R) + \langle A|\,\mathscr{T}_N|D\rangle||\bar{w}_D\rangle \qquad (5)$$

and

$$\lambda(R) = \langle A|\mathscr{H}^{\mathrm{el}}|D\rangle \qquad (6)$$

The extradiagonal terms can be further simplified by making the reasonable assumption that

$$\lambda(R) \gg \langle A|\,\mathscr{T}_N|D\rangle \qquad (7)$$

Furthermore, since ET takes place in a small region of nuclear coordinates, see *infra*, the dependence of the electronic coupling term $\lambda(R)$ on the nuclear coordinates can be safely neglected, leading to the well-known result that the off-diagonal terms of the Hamiltonian matrix are

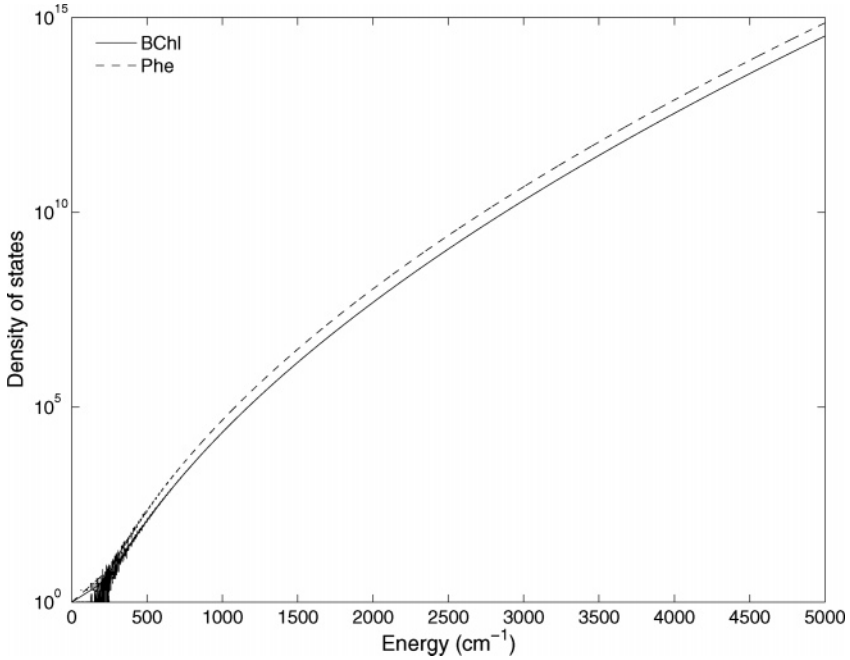

Figure 1. Total density of vibrational states vs energy for the pairs B_A^-/B_A and H_A^-/H_A, computed by using the Beyer−Swinehart algorithm,[31,32] and the vibrational frequencies computed at DFT level.

proportional to the overlap of the vibrational states of $\overline{|A\rangle}$ and $\overline{|D\rangle}$, the so-called Franck-Cordon integrals:

$$H_{A\bar{w}D\bar{v}} = \lambda\langle\bar{v}_A|\bar{w}_D\rangle \tag{8}$$

ET Active Modes. In a hierarchic order of the different effects which could affect ET dynamics in biosystems, the nuclear modes of vibration of the two molecules which exchange an electron should be considered first. In the present study, we will consider only intramolecular modes and will show that, in the case of ET from B_A^- to H_A, the density of coupled states provided by the intramolecular modes of the two redox partners is sufficient to give transition times for ET in very good agreement with the observed one.

Obviously, for judging the importance of intramolecular modes in the ET process, the whole set of normal modes of the pairs $B_A^-H_A$ and $B_AH_A^-$ have to be properly taken into account in dynamics. The methodology employed here has been specifically designed for using the whole set of normal coordinates of the two redox cofactors;[23] it takes into account all the intramolecular effects which can be important for ET, that is, displacements of the equilibrium coordinates, mixing of the normal modes (Duschinsky effect), and changes in vibrational frequencies. The effects of the surrounding medium are neglected in our dynamic approach. These effects are certainly important, since they account both for energy detuning and for wavefunction dephasing. Detuning is crucial in slow ET, as it happens in intersystem crossing, where the coupling between the vibronic level is so small that tight degeneracy conditions are required.[24,25] However, in the case of the ET rate being faster than relaxation of the surrounding medium, it is legitimate, at least as a first approximation, to invoke the adiabatic theorem and treat ET keeping fixed all the slower coordinates. If this approximation does not work for the system in hand, one should find either that the computed probability for ET is vanishingly small or that it becomes vanishingly small by slightly changing the electronic energy difference between the two states. In our case, probabilities for ET computed for different values of the electronic energy difference between the two diabatic states all approach unity, see *infra*, thus confirming the reliability of the adiabatic separation of intramolecular and intermolecular modes for the case in hand. Furthermore, in the case under consideration, the effect of the protein on the electron-transfer rates is negligible; both experimental and theoretical works have shown that the reorganization energy of the protein is relatively small in the case of photosynthetic reaction centers.[26−30] As concerns dephasing, the use of the whole set of the normal coordinates of the redox molecular pairs allows to partially include the faster dephasing effects, inasmuch as there would be several final states, with different vibrational frequencies, which are populated in the electronic transition. That makes the recurrence times much longer than the transition time, leading to dynamics which are essentially irreversible, see *infra*.

In a discrete state approach to ET dynamics, the selection of the vibronic states to be used in the time evolution is probably the most important problem to deal with. In fact, as shown in Figure 1, the density of the vibrational states increases very rapidly as the internal energy increases. For large molecules, such as bacteriochlorophyll and bacteriopheophytin, the density of vibrational states is about 10^5 at $E_{\text{int}} = 1000$ cm^{-1}, computed by using the Beyer−Swinehart algorithm,[31,32] but when the two molecules are considered together (not shown in Figure 1), it increases up to 10^{40}! Obviously a selection of the most important state for ET dynamics becomes mandatory.

The assumptions that the nuclear dependence of the electronic coupling term can be neglected allows to easily identify the active modes for the ET process, namely, those modes whose quantum number can change during the

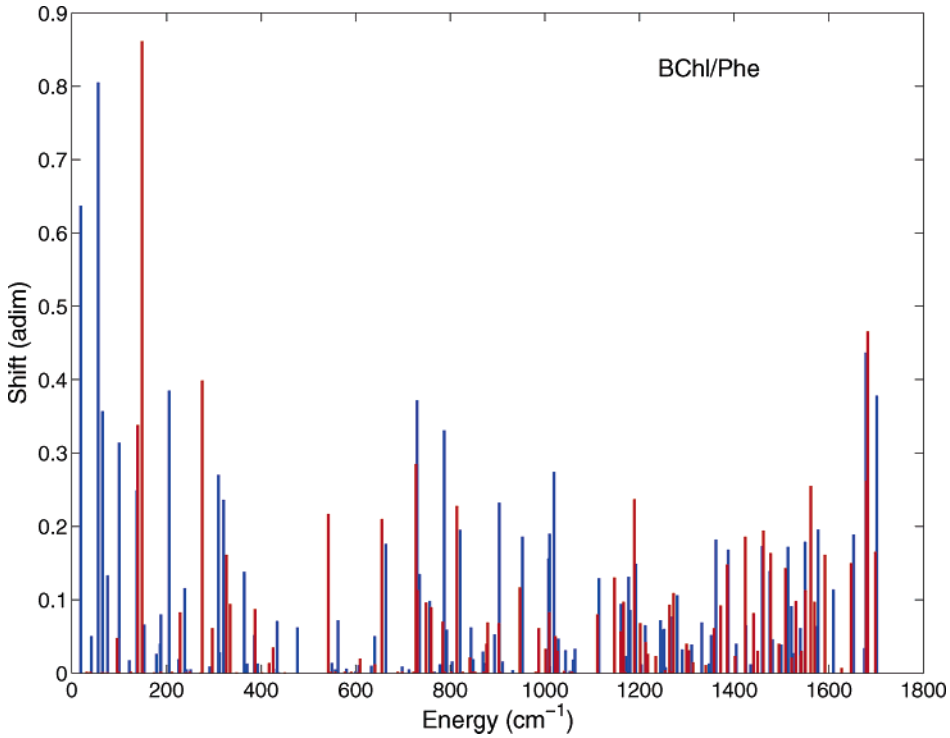

Figure 2. Displaced modes of bacteriochlorophyll (blue) and bacteriopheophytin (red). Absolute values of displacements in adimensional units.

electronic transition. FC integrals between vibronic states with different quantum numbers are vanishingly small whenever changes in population are associated to normal coordinates whose equilibrium positions or directions are the same in the two electronic states. Thus, since the coupling term is proportional to the Franck−Condon integral, eq 8, only displaced or rotated normal modes can give significant FC integrals; all other modes will act as spectators in dynamics since their quantum numbers will be frozen to the initial values.

The displaced and mixed modes can be determined by Duschinsky's normal mode transformation, a fundamental tool for understanding mechanistic details of both radiative and radiationless photochemical processes in polyatomic molecules.[33] Duschinsky's transformation allows expression of the normal modes of vibration of an electronic state of a given molecule in terms of the normal modes of another electronic state, a necessary step for the computation of the Franck−Condon integrals, and provides valuable information about modes which change their equilibrium positions and modes which are mixed with each other for the effect of the electronic transition. Displaced and, to a lesser extent, mixed modes determine the shape of the absorption bands and the dynamics of radiationless processes.

Let $\mathbf{Q}_A$ and $\mathbf{Q}_D$ be the normal mode vectors of a molecule in the electronic states $|A\rangle$ and $|D\rangle$, respectively. According to Duschinsky, the two sets of normal coordinates are related by the expression

$$\mathbf{Q}_A = \mathbf{J}\mathbf{Q}_D + \mathbf{K} \tag{9}$$

where $\mathbf{J}$ is a rotation matrix and $\mathbf{K}$ a displacement vector; the former accounts for mixing of the normal modes upon electronic transition, the latter for changes in the nuclear equilibrium configurations.

If $\mathbf{Q}_A$ and $\mathbf{Q}_D$ are expressed in terms of Cartesian coordinates ξ, which is the most convenient representation for small equilibrium displacements,

$$\mathbf{Q}_\alpha = \mathbf{T}_\alpha^+ \mathbf{m}^{1/2}(\xi - \xi_\alpha^0) \qquad \alpha = A, D \tag{10}$$

then

$$\mathbf{J} = \mathbf{T}_A^+ \mathbf{m}^{-1} \mathbf{T}_D, \qquad \mathbf{K} = \mathbf{T}_A^+ \mathbf{m}^{-1/2}(\xi_D^0 - \xi_A^0) \tag{11}$$

where $\mathbf{m}$ is the diagonal matrix of the atomic masses and $\mathbf{T}_\alpha$ and ξ_α^0 are the normal mode matrix and the equilibrium position vector of the electronic state $|\alpha\rangle$.

In the case where the two electronic states exhibit large equilibrium geometry differences, the normal mode transformation in the Cartesian representation can differ from eq 9 because of the necessary fulfilling of the Eckart conditions in both electronic states (the so-called axis-switching effect);[34] in some cases, the internal coordinate representation can be more convenient than the Cartesian ones; for more details see ref 35.

3. Results

Displaced Modes and Franck−Condon Integrals. The most significant components of the $\mathbf{K}$ vectors and of the $\mathbf{J}$ matrices for B_A^-/B_A and H_A^-/H_A are reported Figure 2 and in Tables 1 and 2, respectively.

Both cofactors possess several modes whose equilibrium positions are significantly displaced upon ET, covering a wide range of wavenumbers, from 25 to 1800 cm^{-1}. Low-frequency modes are important for achieving tight degen-

Table 1. Progressive Normal Mode Number, Wavenumbers (cm^{-1}), and Mixing Coefficients of the Most Mixed[a] Normal Modes of the Pair B_A^-/B_A

	wavenumber		**J**[b]
mode	B_A^-	B_A	$B_A^- \rightarrow B_A$
1	19.4	32.5	−0.78(1) − 0.30(2) − 0.42(4) + 0.29(5)
2	40.8	49.9	−0.60(1) + 0.59(2) + 0.43(4) − 0.26(5)
3	55.7	62.8	0.74(2) − 0.54(4) + 0.28(5)
5	75.7	77.6	0.51(4) − 0.84(5)
113	1652.5	1657.2	−0.34(113) + 0.87(114)
115	1678.7	1690.1	−0.33(113) + 0.32(114) − 0.50(115) +
116	1701.4	1724.0	0.26(113) − 0.81(115) − 0.49(116)
121	3041.9	3066.6	−0.32(120) − 0.77(122) + 0.49(125) +

[a] Only mixed modes with maximum coefficient lower than 0.85. [b] Numbers in parentheses refer to the modes of B_A.

Table 2. Progressive Normal Mode Number, Wavenumbers (cm^{-1}), and Mixing Coefficients[a] of the Most Mixed Normal Modes of the Pair H_A^-/H_A

	frequency		**J**[b]
mode	H_A^-	H_A	$H_A^- \rightarrow H_A$
1	28.41	32.63	0.64(1) + 0.68(2) + 0.16(3) − 0.15(4) + 0.23(5) − 0.15(7)
2	34.45	48.46	−0.76(1) + 0.57(2) + 0.11(3) − 0.15(4) + 0.22(5)
3	57.45	67.36	0.40(2) − 0.14(3) + 0.52(4) − 0.73(5)
4	67.44	70.02	−0.14(2) + 0.96(3) − 0.20(5)
5	74.34	81.45	0.82(4) + 0.55(5)
46	794.93	810.15	0.71(47) − 0.43(48) 0.52(54) − 0.10(57) + 0.11(58)
48	810.86	834.01	−0.37(47) − 0.44(48) + 0.20(50) + 0.50(51) + 0.18(54) + 0.56(55)
49	823.66	839.86	0.48(47) + 0.50(48) + 0.43(50) + 0.43(51) − 0.27(54) + 0.21(55)
50	830.85	842.93	−0.18(47) + 0.52(48) − 0.15(50) + 0.19(51) + 0.74(54) − 0.23(58)
52	837.68	863.70	0.64(50) − 0.59(51) + 0.21(54) + 0.16(55) + 0.20(57) − 0.30(60)
53	851.35	865.04	0.13(47) + 0.19(48) − 0.32(50) − 0.33(51) + 0.73(55) − 0.40(57)
54	852.54	867.25	0.82(52) − 0.56(53)
55	857.43	882.85	−0.55(52) − 0.82(53)
57	875.63	904.07	+0.21(48) + 0.14(51) + 0.12(54) − 0.29(57) + 0.88(58)

[a] Only mixed modes with maximum coefficient lower than 0.85. [b] Numbers in parentheses refer to the modes of H_A.

eracy between initial and final vibronic states, which is a necessary condition for tunneling. High-frequency modes are also very important because they make it possible to fill up large electronic energy gaps between the initial and final states with a modest increase in vibrational quantum numbers.

As to rotated modes, there are important differences between the two pairs. In B_A/B_A^-, there are three groups of significantly mixed modes, most of which are also displaced. The first group includes the lowest frequency modes, which are also the most displaced modes of the B_A^-/B_A pair; they will be therefore used in dynamic simulations. The other two groups include modes at a higher frequency, whose excitation lead to energies higher than that of the ground vibronic state of $\overline{|B_A^- H_A\rangle}$, which we will assume to be the only state populated at $t = 0$. Thus, these groups of rotated modes will not be used in dynamics.

By contrast, H_A exhibits a large number of mixed modes in a wide region of wavenumbers, which can be grouped into four subsets. The first group includes the five lowest-frequency modes; the second one consists of 12 modes spanning the region from 794 to 886 cm^{-1}, cf. Table 2; the last two groups, not reported in Table 2, include eight modes, from 1088 to 1191 cm^{-1}, and 13 modes, falling in the wavenumber range 1327−1509 cm^{-1}. The first group of rotated modes can be potentially useful in dynamics for fine energy tuning; all other modes fall at too high a frequency for this purpose, and since the FC integrals between rotated modes with different quantum numbers are much lower than those obtained from displaced modes, they will be discarded in dynamics.

The FC integrals between the ground vibronic state of $\overline{|B_A^- H_A\rangle}$ and a selected small fraction (ca. 2×10^{13}) of $\overline{|B_A H_A^-\rangle}$ are shown in Figure 3, as a function of the vibrational energy of the final states. The vibrational modes of $\overline{|B_A H_A^-\rangle}$ which have been excited in computation and the maximum number of states for each mode are specified in the caption of Figure 3.

The inset of Figure 3 shows a magnification over a tiny energy region corresponding to the experimental free-energy change upon ET, ca. 1300 cm^{-1}. Since in the model adopted here the coupling between vibronic states is proportional to FC integrals, Figure 3 provides a picture of the relative values of the extra-diagonal row of the Hamiltonian matrix ($\mathbf{H}_{AD}$ of eq 3) as a function of the vibrational energy of the final state. There is a very dense manifold of final vibronic states which are coupled to the initial ground vibronic state; the hole appearing between 800 and 1000 cm^{-1} is an artifact due to our choice of the excitation numbers used in computation, which have been made for favoring the energy region around 1300 cm^{-1}, corresponding to the electronic energy difference between $|B_A^- H_A\rangle$ and $|B_A H_A^-\rangle$. These results would suggest that, provided that small energy fluctuations, much smaller than a thermal quantum $k_B T$ (k_B is the Boltzmann constant), take place, ET from B_A^- to H_A can be mechanistically modeled as a nonradiative transition which mainly involves the intramolecular modes of vibration of the two redox cofactors, without the assistance of the low-frequency modes of the medium, in agreement with the general finding that the rates of most of the ET processes occurring in photosynthetic reaction centers are only moderately temperature-dependent.[26,27,36−38]

Energy Parameters and Electronic Coupling Elements. The relative energy of the two electronic states (including the zero-point contribution) has been determined by spectroscopic measurements. The free energy level of the intermediate charge-separated state was found ca. 500 cm^{-1}

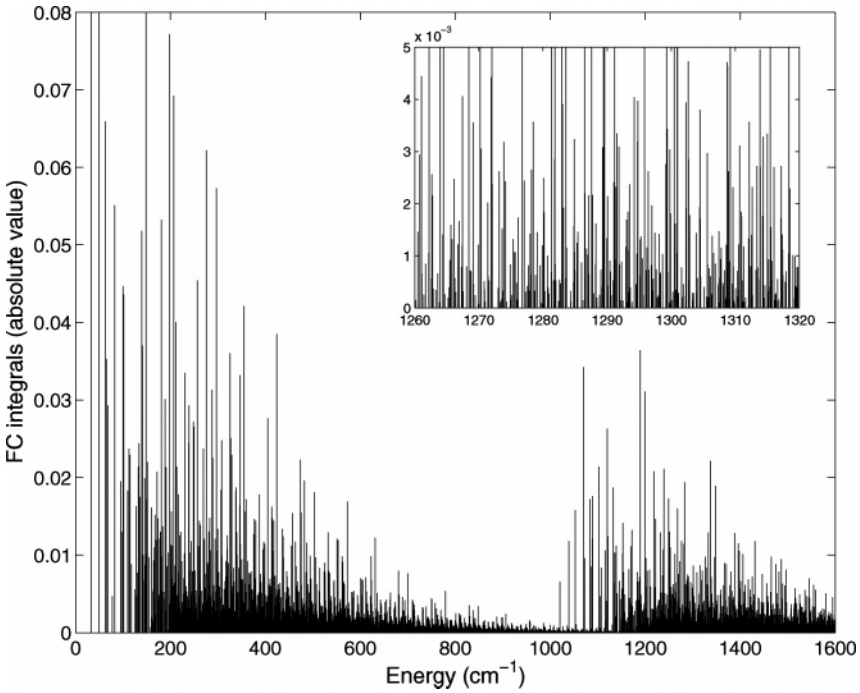

Figure 3. Franck−Condon integrals (absolute value) as a function of the vibrational energy (cm^{-1}) of the final states between the vibronic states of $|B_A^- H_A\rangle$ and a selected large fraction of the manifold of $|\overline{B_A H_A^-}\rangle$ including the following modes (numbers in parentheses indicate the maximum quantum number allowed in computation): B_A {135.48(3), 146.22(5), 225.01(2), 277.64(2) 297.92(1), 386.37(2), 529.85(2), 659.67(2), 724.18(2), 730.64(2), 761.60(2), 788.83(2), 1281.39(2), 1691.72(2), 1761.78(2)}; H_A, {76.41(2), 86.16(1), 128.06(1), 206.90(2), 318.45(1), 367.50(4), 473.29(6), 1000.67(1), 1083.25(1), 1167.06(1), 1174.46(4), 1447.34(2), 1494.19(3), 1545.19(3), 1643.85(1)}.

below that of P*, while the energy difference between P* and the state $P^+H_A^-$ is ca. 1800−1900 cm^{-1}.[39]

As concerns the electronic coupling element, both the size of the system and the lack of symmetry rule out the possibility of computing that parameter by ab initio configuration interaction computations. It has been shown in the past that, while semiempirical methods do not provide sufficiently accurate estimates for the electronic coupling,[40,41] the recourse to ab initio Hartree−Fock computations gives values which are in reasonable agreement with those obtained by reasonable fitting of the experimental ET rates.[42] Reliable estimates of electronic coupling elements can also be obtained from the widely accepted exponential dependence of the electronic coupling element on the distance between the donor and acceptor sites. We have used Hopfield's expression:[9]

$$H_{lm} = \frac{2.7}{\sqrt{N_a N_b}} \exp(-\beta R_{lm}) \qquad \text{in eV} \tag{12}$$

where R is the edge-to-edge distance between two large aromatics of N_a and N_b atoms.

The X-ray structure of the PRC from *Rhodobacter sphaeroides*[43] indicates that the edge-to-edge distance between B_A and H_A is ca. 4.5 Å. The parameter β has been estimated by taking as a reference the values of the electronic coupling elements between quinones in bacterial PRC, evaluated as half of the energy difference of the two adiabatic states in a point of the avoided crossing region.[44] The ab initio multireference configuration interaction value (17 cm^{-1}) yields $\beta = 0.49$ Å^{-1}, a value slightly lower than that suggested by Hopfield (0.72)[9] but in line with other values reported in the literature.[45] With that value of β, the coupling factor for ET between B_A^- and H_A is ca. 90 cm^{-1}, in very good agreement with ab initio Hartree−Fock computation.[42] This point is important because the transition times for ET crucially depend on that parameter.

Transition Probabilities. The Franck−Condon integrals reported in Figure 3 show that there is a dense manifold of vibronic states of $|B_A H_A^-\rangle$ which are coupled to the vibronic ground state of $|B_A^- H_A\rangle$. However, since only a few FC integrals are significantly high, for most of the states of $|\overline{B_A H_A^-}\rangle$, the coupling term with the initial state is small. We have therefore first investigated the effects of small change in the electronic energy difference (ΔE_{el}) between $|B_A^- H_A\rangle$ and $|B_A H_A^-\rangle$ on the transition probabilities. Several time propagations have been carried out, starting with $\Delta E_{el} = 1300$ cm^{-1} and exploring an energy range of ±50 cm^{-1} around this value, without attempting to optimize the active space for each energy point. In all the cases, the transition probabilities for ET approach to unity, thus assuring that the results are not due to the occurrence of a few accidental degeneracies but rather to the existence of a Franck−Condon weighted density of states sufficiently high to promote ET.

The results of some dynamic simulations are displayed in Figure 4, for values of ΔE_{el} in the range 1265−1315 cm^{-1}, by varying each time ΔE_{el} by 5 cm^{-1}. The space of the active modes used in computations is reported in the caption of Figure 4. The transition probabilities reported in Figure 4 are summed over the whole vibrational manifold of $|B_A H_A^-\rangle$. For most values of ΔE_{el}, the initial state irreversibly decays

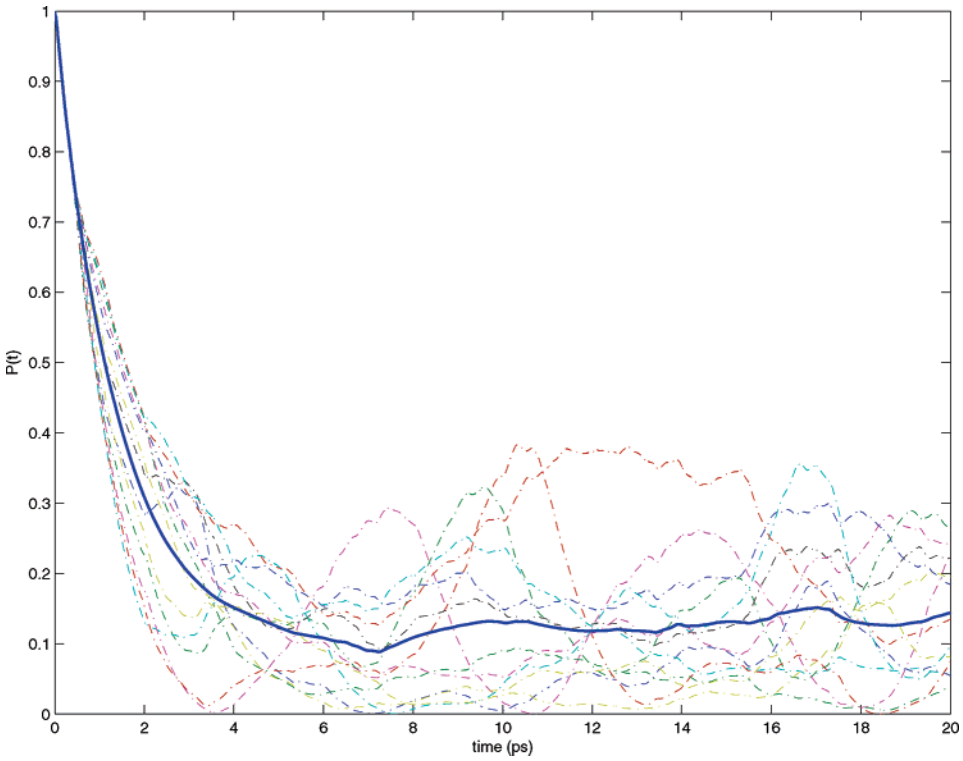

Figure 4. Transition probabilities for ET from B_A to H_A for different values of ΔE_{el}, see text, and their average (thick line). Excited modes (wavelength-maximum excitation): B_A (67.94−2, 77.66−2, 101.51−2, 141.02−2, 206.62−2, 238.65−2, 1020.24−1, 1039.37−1, 1199.50−1, 1282.95−1); H_A^- (139.03−2, 148.44−2, 275.64−2, 326.77−1, 1189.63−1, 1271.98−1).

in the manifold of $\overline{|B_A H_A^-\rangle}$, within 2−5 ps. In a few cases, the population shows a few damped oscillations which rapidly decay in a few tens of picoseconds. The Boltzmann average of all decay curves (the thick line of Figure 4) has been fitted with an exponential function, from which an average half-transition time of 1 ps has been obtained, in very good agreement with the experimental observation.

4. Conclusion

The results presented in this paper indicate that ET from B_A^- to H_A in photosynthetic reaction centers can be successfully modeled as a nonradiative transition which mainly involves the intramolecular modes of vibration of the two redox cofactors. Thus, a physical model in which the role of the surrounding medium is that of accounting for small energy fluctuations—simulated here by performing an average of the transition probabilities over a tiny interval of ΔE_{el} caused by weak interactions of the two redox partners with their environments—appears to be able to correctly reproduce the rate of ET from chlorophyll to pheophytin in bacterial reaction centers.

The above conclusion of course holds for the specific case of ET considered here, but analyses such as that used here, based on a detailed knowledge of the intramolecular modes of vibration of the two redox cofactors, can be also useful for a better understanding of cases where the embedding medium is known to play a major role.

5. Computational Details

Equilibrium geometries, normal modes, and vibrational frequencies of bacteriochlorophyll and bacteriopheophytin in their neutral and anionic forms were obtained at the DFT level using the standard B3LYP functional with a 6-31G-(d,p) basis set. In order to obtain reliable estimates of these quantities, we have preferred to compute them for the isolated redox cofactors in the gas phase by using the highest level of computation compatible with the size of the molecules. Of course, quantum mechanics/molecular mechanics methods could be employed for taking into account the effects of the environment, but at the present stage of development, these methods are well-suited only for considering steric effects, which are not expected to play any role in fast ET. Reliable polarizable force fields, which could account for electronic stabilization of ionic states, are not yet available.

The dynamics of ET have been determined by solving the time-dependent Schrödinger equation using a Chebyshev algorithm, with the initial condition that at $t = 0$ only the vibronic ground state of $|B_A^- H_A\rangle$ is populated. As concerns the final states, the vibronic states of $|B_A H_A^-\rangle$ obtained by exciting 19 vibrational normal modes, 13 from chlorophyll and 6 from pheophytin, have been considered in dynamic computations. More than 2×10^8 vibronic states of $\overline{|B_A H_A^-\rangle}$ have been initially considered. The evaluation of the FC integrals between the vibronic ground state of $|B_A^- H_A\rangle$ and the selected manifold of $\overline{|B_A H_A^-\rangle}$ has been carried out by using the MOLFC program,[46] which is based on the recurrence relations reported in ref 47.

The manifold of vibronic states of $|B_A H_A^-\rangle$ has been further pruned by considering only those states whose energy differences with the initially populated state (ΔE_{if}) and couplings V_{if} satisfy the criterion $|V_{if}/\Delta E_{if}| > \epsilon$, where ϵ is a

properly chosen small number (10^{-4} in our case); the resulting vibronic space includes more that 15 000 states.

The modes included in the active space and the number of states for each mode have been selected on the basis of several test computations, which also indicate that there are other modes potentially important for ET. Further investigations and improvements of the model are in progress.

Acknowledgment. A.P. is pleased to dedicate this paper to Dennis Salahub as a token of his esteem and friendship; he will always remember the marvelous days spent in Montreal in Dennis' group. The financial support of the Italian Ministry of University and of the University of Salerno is gratefully acknowledged.

References

(1) Feher, G.; Allen, J. P.; Okamura, M. Y.; Rees, D. C. *Nature* **1989**, *339*, 111.

(2) Kuhn, H. *Phys. Rev. A: At., Mol., Opt. Phys.* **1986**, *34*, 3409−3425.

(3) Gust, D.; Moore, T. A.; Moore, A. L. *Acc. Chem. Res.* **1993**, *26*, 1988.

(4) Gratzel, M. *Acc. Chem. Res.* **1981**, *14*, 376.

(5) Ballardini, R.; Balzani, V.; Credi, A.; Gandolfi, M. T.; Venturi, M. *Acc. Chem. Res.* **2001**, *34*, 445.

(6) Gust, D.; Moore, T. A.; Moore, A. L. *Acc. Chem. Res.* **2001**, *34*, 40−48.

(7) Kodis, G.; Terazono, Y.; Liddell, P.; Andreasson, J.; Garg, V.; Hamburger, M.; Moore, T. A.; Moore, A. L.; Gust, D. *J. Am. Chem. Soc.* **2006**, *128*, 1818−1827.

(8) Marcus, R. A. *J. Chem. Phys.* **1956**, *24*, 966−978.

(9) Hopfield, J. J. *Proc. Natl. Acad. Sci. U.S.A.* **1974**, *71*, 3640−3644.

(10) Kestner, N. R.; Logan, J.; Jortner, J. *J. Phys. Chem.* **1974**, *78*, 2148−2166.

(11) Sumi, H.; Marcus, R. A. *J. Chem. Phys.* **1986**, *84*, 4894−4914.

(12) Markel, F.; Ferris, N.; Gould, I.; Myers, A. *J. Am. Chem. Soc.* **1992**, *114*, 6208−6219.

(13) Fischer, S. F.; Van Duyne, R. P. *Chem. Phys.* **1977**, *26*, 9−16.

(14) Schenck, C. C.; Parson, W. W.; Holten, D.; Windsor, M. W.; Sarai, A. *Biophys. J.* **1981**, *36*, 479−489.

(15) Borrelli, R.; Di Donato, M.; Peluso, A. *Biophys. J.* **2005**, *89*, 830−841.

(16) Mlynarski, P.; Salahub, D. *Phys. Rev. B: Condens. Matter Mater. Phys.* **1990**, *43*, 1399.

(17) Jamorski, C.; Casida, M.; Salahub, D. *J. Chem. Phys.* **1996**, *104*, 5134.

(18) Casida, M.; Jamorski, C.; Casida, K.; Salahub, D. *J. Chem. Phys.* **1998**, *108*, 4439.

(19) Casida, M.; Salahub, D. *J. Chem. Phys.* **2000**, *113*, 8918.

(20) Martin, J. L.; Breton, J.; Hoff, A. J.; Migus, A.; Antonetti, A. *Proc. Natl. Acad. Sci. U.S.A.* **1986**, *83*, 957−961.

(21) Arlt, T.; Schmidt, S.; Kaiser, W.; Lauterwasser, C.; Meyer, M.; Scheer, H.; Zinth, W. *Proc. Natl. Acad. Sci. U.S.A.* **1993**, *90*, 11757−11761.

(22) Robinson, G. W.; Frosch, R. P. *J. Chem. Phys.* **1963**, *38*, 1187.

(23) Borrelli, R.; Peluso, A. *J. Chem. Phys.* **2003**, *119*, 8437−8448.

(24) Landau, L. *Phys. Z. Sowjetunion* **1932**, *2*, 1695.

(25) Zener, C. *Phys. Rev.* **1929**, *33*, 536.

(26) Gunner, M. R.; Robertson, D. E.; Dutton, P. L. *J. Phys. Chem.* **1986**, *90*, 3783−3795.

(27) Gunner, M. R.; Dutton, L. P. *J. Am. Chem. Soc.* **1989**, *111*, 3400−3412.

(28) Parson, W.; Warshel, A. *J. Phys. Chem. B* **2004**, *108*, 10474−10483.

(29) Warshel, A.; Chu, Z. T.; Parson, W. W. *Science* **1989**, *246*, 112−116.

(30) Parson, W. W.; Chu, Z. T.; Warshel, A. *Biophys. J.* **1998**, *74*, 182−191.

(31) Beyer, T.; Swinehart, D. F. *Commun. Assoc. Comput. Machin.* **1973**, *16*, 379.

(32) Stein, S. E.; Rabinovitch, B. S. *J. Chem. Phys.* **1973**, *58*, 2438−2445.

(33) Duschinsky, F. *Acta Physicochim. URSS* **1937**, *7*, 551−566.

(34) Houghen, J. T.; Watson, J. K. G. *Can. J. Phys.* **1965**, *43*, 298.

(35) Borrelli, R.; Peluso, A. *J. Chem. Phys.* **2006**, *125*, 194308.

(36) Woodbury, N. W. T.; Becker, N.; Middendorf, D.; Parson, W. W. *Biochemistry* **1985**, *24*, 7516−7521.

(37) Kirmaier, C.; Holten, D.; Parson, W. W. *Biochim. Biophys. Acta* **1985**, *810*, 33−48.

(38) McElroy, J. D.; Mauzerall, D. C.; Feher, G. *Biochim. Biophys. Acta* **1974**, *333*, 261−278.

(39) Yakovlev, A. G.; Shkuropatov, A. Y.; Shuvalov, V. A. *Biochem.* **2002**, *41*, 2667−2674.

(40) Warshel, A.; Creighton, S.; Parson, W. W. *J. Phys. Chem.* **1988**, *92*, 2696−2701.

(41) Plato, M.; Mobius, K.; Michel-Beyerle, M. E.; Bixon, M.; Jortner, J. *J. Am. Chem. Soc.* **1988**, *110*, 7279.

(42) Zhang, L. Y.; Friesner, R. A. *Proc. Natl. Sci. U.S.A.* **1998**, *95*, 13603.

(43) Stowell, M. H. B.; McPhillips, T.; Rees, D. C.; Soltis, S. M.; Abresch, E.; Feher, G. *Science* **1997**, *276*, 812−816; PDB ID: 1AIG.

(44) Di Donato, M.; Peluso, A.; Villani, G. *J. Phys. Chem. B* **2004**, *108*, 3068−3077.

(45) Almeida, R.; Marcus, R. A. *J. Phys. Chem.* **1990**, *94*, 2978−2985.

(46) Borrelli, R.; Peluso, A. *MolFC: A Program for Franck−Condon Integrals Calculation*; Theoretical Chemistry Group, University of Salerno: Salerno, Italy, **2006**. Package available free of charge at http://www.theochem.unisa.it.

(47) Peluso, A.; Santoro, F.; Del Re, G. *Int. J. Quantum Chem.* **1997**, *63*, 233−244.

CT6003802